POLITECNICO DI TORINO
Repository ISTITUZIONALE

Assessing the effect of modelling approaches for longitudinal train dynamics simulations with a multibody code

Original
Assessing the effect of modelling approaches for longitudinal train dynamics simulations with a multibody code / Magelli, M., Correa, P.H.A., Santos, A.A.D.. - In: PROCEEDINGS OF THE INSTITUTION OF MECHANICAL ENGINEERS. PROCEEDINGS PART K, JOURNAL OF MULTI-BODY DYNAMICS. - ISSN 1464-4193. - 239:4(2025), pp. 326-338. [10.1177/14644193251368540]

Availability:
This version is available at: 11583/3008069 since: 2026-03-05T13:28:16Z

Publisher:
SAGE Publications Ltd

Published
DOI:10.1177/14644193251368540

Terms of use:

This article is made available under terms and conditions as specified in the corresponding bibliographic description in the repository

Publisher copyright
Sage postprint/Author's Accepted Manuscript

Magelli, M.; Correa, P. H. A.; Santos, A. A. D., Assessing the effect of modelling approaches for longitudinal train dynamics simulations with a multibody code, accepted for publication in PROCEEDINGS OF THE INSTITUTION OF MECHANICAL ENGINEERS. PROCEEDINGS PART K, JOURNAL OF MULTI-BODY DYNAMICS (239 4) pp. 326-338. © 2025 (Copyright Holder). DOI:10.1177/14644193251368540

(Article begins on next page)

11 November 2026

Assessing the effect of modelling approaches for longitudinal train dynamics simulations with a multibody code

Authors: M. Magelli[a], P. H. A. Correa[b]*, and A. A. Santos[b]

a) Department of Mechanical and Aerospace Engineering, Politecnico di Torino, C.so Duca degli Abruzzi 24, 10129, Torino, Italy

b) Railway Laboratory (Lafer), Universidade Estadual de Campinas (UNICAMP), Campinas, SP, Brazil

*corresponding author: Pedro H. A. Correa, e-mail: p263135@dac.unicamp.br, Tel.: +5524992243596

Abstract

Different methods can be used to incorporate longitudinal train dynamics (LTD) into multibody (MB) models, which is crucial for understanding the dynamic behaviour of railway vehicles. The main contribution of the paper is to test and compare different strategies under the same simulation scenario, involving a group of four wagons with three-piece bogies. Some strategies are based on data exchange between MB and LTD frameworks, while others are purely standalone MB models including LTD states. The study confirms that all strategies can yield similar results, but they differ significantly in computational efficiency. Modelling vehicles as masses with a single degree of freedom (DOF) within the MB environment is 6.5 times slower than running a MB simulation with in-train forces from a preliminary LTD simulation. On the other hand, co-simulation performs poorly, mainly due to the chosen communication rate between LTD and MB codes. When an optimal data exchange rate is selected, computational speeds can decrease by about three orders of magnitude in the reference scenario. A balanced solution can be achieved by modelling wagon sets with large masses inside the MB framework, reducing the number of DOFs and thus achieving computational speeds comparable to those of the straightforward methods.

Keywords: longitudinal train dynamics; multibody system dynamics; running safety; co-simulation; three-piece bogie; heavy haul wagon

1. Introduction

Train dynamics is generally categorized into two main domains: longitudinal train dynamics (LTD) and multibody dynamics. The first concerns the analysis of in-train forces and the motion of each vehicle along the direction of travel, including phenomena such as traction, braking, and coupler interactions, without considering the interaction of each body in the vehicle itself. In contrast, multibody dynamics involves the vehicle's motion both along and perpendicular to the track and is inherently more complex. This complexity comes from the necessity of accurately modelling the nonlinearities of wheel-rail contact problems and forces transmitted through the suspension system at all levels. Capturing these interactions requires multibody dynamic models (MB) and advanced numerical methods as lateral instabilities, hunting motion, and curving behaviour critically influence ride quality and safety. [1]

LTD codes generally account for each car using a single degree of freedom (DOF) model that follows the track layout with the application of resistance forces emulating curvature and slope. On the other hand, studies on multibody dynamics are usually performed in MB system codes with multiple bodies, multiple DOFs and a track layout accounting for curvature, slopes, and irregularities. As MB models feature 6 DOFs (translation and rotation in three directions each), this model is called full dynamics. The combination of those areas for a comprehensive dynamic model is possible, accounting for the full dynamics of an isolated vehicle and its interaction with the rest of the composition, including in-car forces from LTD analysis, although higher computational power is needed. [2,3]

Obviously, as LTD only considers a limited subset of coordinates in the dynamic simulation of railway vehicles, it could be possible to develop LTD models within MB frameworks, provided that all other coordinates are properly constrained. This was done by Bosso et al. [4], who built a SIMPACK model including both detailed wagons, with may DOFs, and simplified ones, with fewer DOFs. Similarly, Correa et al. [5] implemented a SIMPACK model of a freight train with 100 wagons modelling 3 pairs of wagons (6 wagons) in detail, while all other vehicles were modelled as bodies with a single DOF along the track. Nonetheless, whilst detailed MB models of railway vehicles are commonly implemented within commercial software packages to investigate their full dynamics [6], LTD models are usually built as in-house routines to improve their computational efficiency, in view of the simplified modelling assumptions. Therefore, for comprehensive dynamic models, it is often required to combine different codes and simulation frameworks. This can raise some concerns about computational efficiency, as MB models usually have poorer performances with respect to LTD models, in view of the larger number of DOFs and strong nonlinearities.

In the past years, different strategies have been developed to combine the benefits of LTD simulations with the MB detailed dynamics of one single vehicle. The most straightforward technique involves the use of two codes separately: one LTD generating in-train forces and then feeding these outputs into an MB standalone model of a single vehicle or small group of vehicles.[7] A different approach is to build a detailed model of a small group of cars trailed by bodies with big inertia and prescribed speed profile, and then calculate the in-train forces inside the group using control elements to model the draft gear nonlinear behaviour. [5]. These approaches are easy to implement but lack the mutual interaction between the long-train forces and the actual behaviour of the vehicle. [3,8]

Co-simulation strategies fix this mutual dependency issue, making it possible to run the LTD simulation feeding the MB model and vice-versa, for each timestep, possibly taking advantage of parallel computing. [9,10] However, the major drawback of this approach relies on the fact that the communication rate between the two codes needs to be high to avoid data loss and delays in the exchange of states, which often causes an increase in computational time. When implementing co-simulation interfaces, a key factor is the selection of the communication protocol. Wu et al. [11] recently showed that for co-simulation between LTD models and pneumatic modules for the simulation of the air brake pipe pressure, the communication overhead times strongly depend on the data exchange protocol. Precisely, the Open Multi-Processing (OpenMP) interface had the smallest overheads, thanks to shared memory, while the TCP/IP protocol had the poorest performances. The Message Passing Interface (MPI) technique had a performance in between the OpenMP and TCP/IP protocols. In their study, Spiryagin et al [12] developed a co-simulation framework between an in-house LTD code and an MB model implemented in the GENSYS commercial code, based on data exchange through the TCP/IP protocol. This approach proved to be up to 6 times slower when compared to the straightforward approach mentioned before.

Nowadays, some commercial MB software packages present LTD modules, such as the longitudinal dynamics module for the non-linear creep solver on Vampire, introduced in 2022. However, this module only allows to specify the coefficients for the calculation of ordinary resistances acting on vehicles modelled in detail inside the code, thus neglecting the rest of the composition. Conversely, the Train3D module on Universal Mechanism (UM) [13] allows to define detailed models for some vehicles in the train composition while modelling the rest of the train as single DOF masses in the framework of LTD codes. The latter method can be implemented within in-house LTD codes, too, as suggested by Cantone et. al [14], but it requires that the numerical integrator used for LTD simulations can effectively solve the wheel-rail contact problem.

Another methodology currently investigated by researchers consists of building the entire composition to evaluate the in-train forces and phenomena within the MB formalism. Bosso et al. [15] created simplified versions of each wagon in the composition with three bodies (one wagon and two bogies) on SIMPACK, but the method proved to be unstable for trains with many wagons. To overcome these issues, Magelli and Zampieri [16] recently suggested solving the LTD of groups of wagons inside the MB environment through the definition of user-defined force elements with associated dynamic states, achieving promising computational performances. However, this is a brand-new method that requires low-level functions to interact with the MB solver, which makes it trickier to implement. Therefore, the present paper only considers and benchmarks traditional approaches.

Moreover, researchers have even started building digital twins of MB/LTD models by deriving closed-form fast-to-evaluate surrogate models with machine learning and artificial intelligence techniques. [17,18] Nonetheless, these on-the-edge approaches are not considered here since they lose information on the physical background of LTD and MB systems when building the surrogate models.

The state-of-the-art provided in the lines above highlights that different strategies exist in the literature to combine LTD and MB simulations. Nonetheless, to the authors' knowledge, the literature lacks a thorough comparison of the different strategies, considering their numerical accuracy, stability, efficiency and impact on the major simulation outputs. Therefore, as a major novelty, this work intends to deeply compare the performances of different existing strategies in the same reference simulation scenario, extracted from the international benchmark of LTD simulators. [19,20] The goal of the paper is to highlight the benefits and drawbacks of each method, discussing several aspects related to practical implementation and numerical issues, as well as investigating possible arising differences in terms of calculated outputs. In fact, in the authors' opinion, this benchmarking activity is needed since in-train forces and their modelling strategies are known to impact the running safety indexes.

The comparison of the tested approaches allows to gain a further understanding of the effects that different LTD strategies have on the major safety indexes calculated using detailed wagons, which are derived from the wheel-rail contact forces. It is believed that the results of the activity shown in the paper can better drive scholars and researchers needing to implement their own framework to combine LTD and MB simulations, providing a detailed overview on the expected outputs and performances of different existing approaches.

The next section presents the SIMPACK model of the reference wagons and track, the scenario used to validate the results, and the explanation of each approach developed to model the composition. Then, the result section shows the validation and comparison of the tested strategies. The final section provides the discussion and conclusions, summarizing the findings of the activity and highlighting the benefits of each approach.

2. Computational framework

2.1 Scenario and SIMPACK Model

The selected scenario for simulations and validation is the "train 4" configuration, as documented in the international benchmark of LTD simulators. This configuration bears similarities to the train setup used in Brazil for freight transportation, particularly the gondola wagons that transport ore from mining operations to coastal ports. The benchmark's "train 4" comprises two "type 2" locomotives, followed by a set of 120 "type 2" freight wagons, a remote "type 1" locomotive, and a tail set of 120 "type 2" wagons. Detailed properties of these vehicles are provided in Table 1.

Table 1 - Measurements for the wagon and the locomotives.

Vehicle	Number of axles	Axle Load (tonne)	Overall length (m)
Type 1 Locomotive	6	22.33	22.95
Type 2 Locomotive	6	32.50	24.35
Type 2 Wagon	4	40.00	11.00

The wagons are grouped in sets of 120 cars, divided into 60 wagon pairs connected by a rigid drawbar with draft gears. The wagon pairs are connected to each other and to the locomotives using couplers with 10 mm of slack. Locomotives are also connected using couplers. Both bars and couplers feature nonlinear mechanical impedance characteristics with hysteresis.

Apart from the data given in Table 1, the international benchmark does not explicitly provide the details of the cars used to inspire the vehicles, so a three-piece bogie gondola wagon is proposed to represent the type 2 wagon. A wagon pair with the relevant dimensions is sketched in Figure 1, which also provides snapshots of the three-piece bogie model implemented in SIMPACK. For brevity, the multibody model built in SIMPACK will be referred to as the MB model. The MB model of the four wagons behind the remote locomotive is built in SIMPACK, starting from existing models developed in past activities [5,21–23]. For each wagon in the MB model, the payload is adjusted to consider the effect of the wheelset rolling inertia. Still, this contribution is negligible to the total vehicle weight on rails. The other dimensions were taken from existing bogies and vehicles with similar characteristics. The vehicle runs on a track with a broad gauge of 1.6 m.

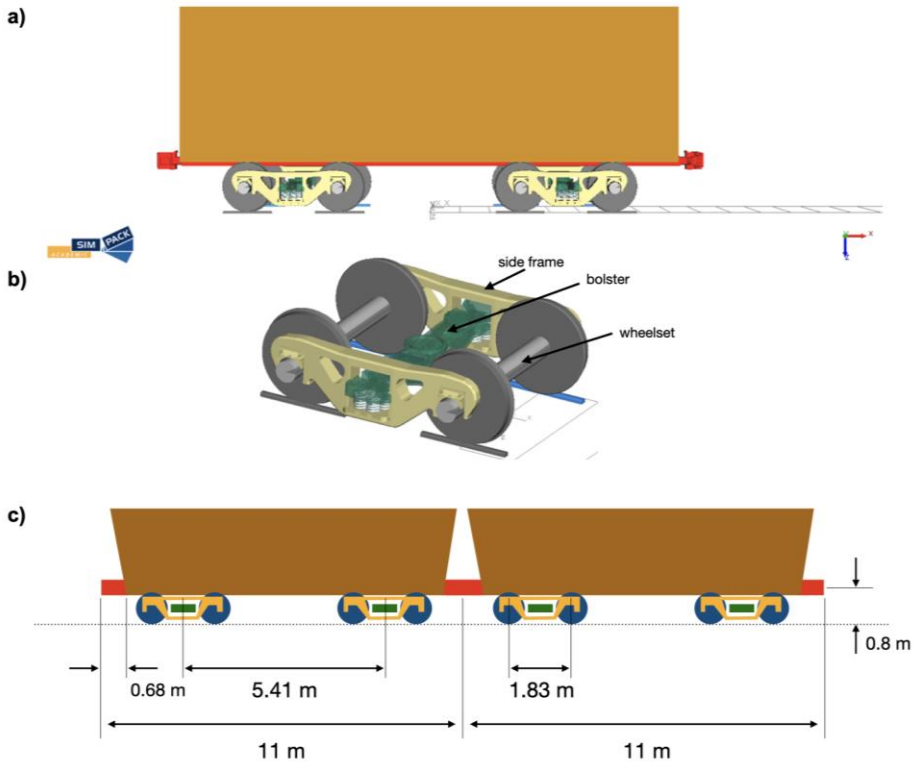

Figure 1 – Model of benchmark type 2 wagon (a) with three-piece bogie (b) and relevant dimensions (c).

The vehicle model totals 11 rigid bodies and 62 DOFs each. The connection between the detailed wagons is obtained with nonlinear hysteresis point-to-point (Ptp) forces, acting purely as traction and compression elements, considering fully nonlinear mechanical impedance characteristics for the coupling elements. For each of the four detailed wagons, the model incorporates an additional force element defined between a moving marker along the track and a marker on the carbody, used to apply the curving and ordinary resistance. Different expressions exist in the literature for the evaluation of the ordinary and curving resistant forces.[24] Usually, ordinary resistances are evaluated as second-order polynomial functions of running speed, while curving resistances are commonly calculated as a function of the curve radius only, although some laws that account for the effect of the unbalanced acceleration exist, too. [25] Nonetheless, since the simulation scenario selected for this paper is extracted from the international benchmark of LTD simulators, the contribution of ordinary and curving resistances is calculated with the following expression, derived from the LTD benchmark paper. [19]

$$F_{res} = \frac{m}{1000} \cdot \left[\left(2.943 + \frac{89.2}{P_{ax}} + 0.00085\dot{S} + \frac{0.0094\dot{S}^2}{P_{ax} n_{ax}} \right) + 6116\psi'(S) \right] \quad (1)$$

where m is the wagon mass, P_{ax} is the axle-load in tonne, $\dot{S}$ is the joint speed state, n_{ax} is the number of axles and finally $\psi'(S)$ is the curvature along the track.

The wheel and rail profiles used for the simulation are new profiles, and the contact problem is addressed using models available in the SIMPACK code. Specifically, the normal problem is solved using an equivalent elastic approach, namely a semi-Hertzian method that converts non-Hertzian contact patches, identified as a function of the relative penetration between wheel and rail, into equivalent ellipses. The tangential contact problem is subsequently solved with the FASTSIM algorithm, which is widely used in railway dynamics simulations and provides a balance between accuracy and computational efficiency.[26,27]

The track used in this work, shown in Figure 2, is the one proposed in the international benchmark of LTD simulators [19] Still, it includes cross-level superelevation data on curves, which were determined considering the prescriptions of Brazilian railways.[28] Since the goal of the present paper is to compare different strategies for the combination of LTD and MB dynamics, rather than investigating in detail the dynamic behaviour of the reference wagons under specific operating conditions, the track is modelled without irregularities. This is done to avoid the effect of stochastic parameters in the comparison of the tested strategies. Furthermore, although line irregularities do have an impact on railway vehicle dynamics, it can be expected that the effect of irregularities would be similar for all modelling strategies shown in this paper.

For all strategies, the simulation time of 3863 s is defined as the stop criteria. This is the time the simulation should take to complete the 50 km of track with the expected speed profile.

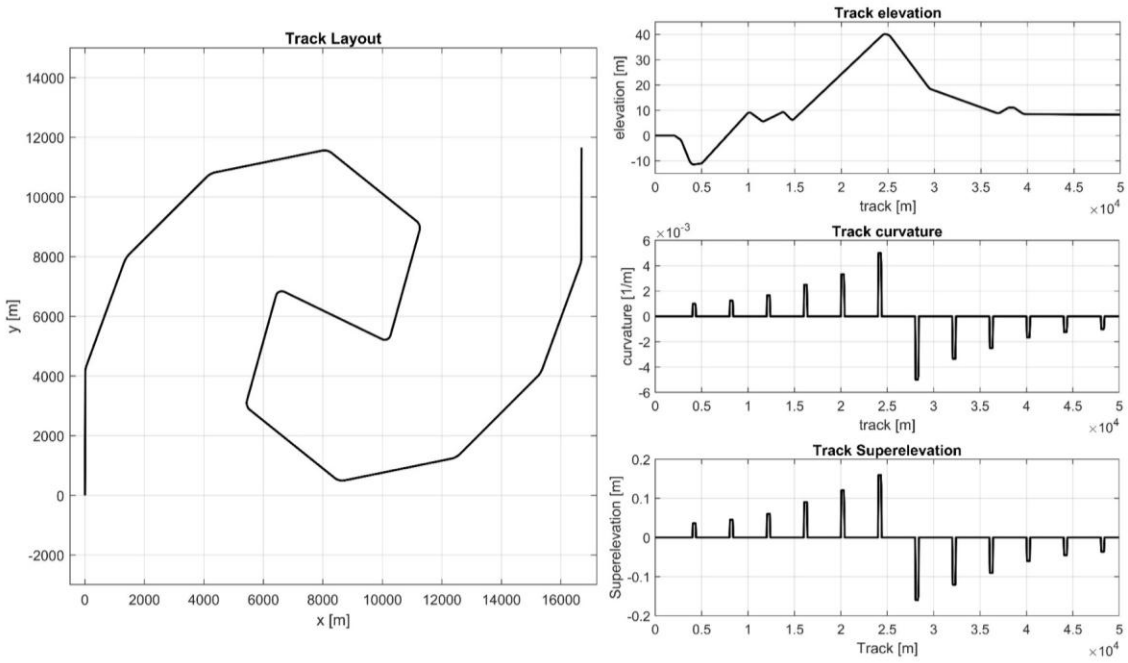

Figure 2 - Track layout, elevation, curvature, and superelevation.

2.2 Strategies for LTD

This paper proposes the comparison among the four strategies that combine the effects of LTD with the benefits of having a 3D MB model, as sketched in Figure 3. The strategies tested in the present paper rely on two base models developed in past activities, namely the MB model of the gondola wagon, described in the previous section, and the LTDPoliTo code developed by the research group from Politecnico di Torino in MATLAB [19] for LTD simulations. The LTDPoliTo code adopted in this work solves the system of ordinary differential equations (ODEs) that describe the longitudinal dynamics of each vehicle in the train composition, which can be written as:

$$m_j \ddot{s}_j = F_{c,j} - F_{c,j-1} + F_{tdb,j} - F_{air,j} - F_{res,j} - F_g \tag{2}$$

where subscript j refers to the j-th vehicle in the train composition, s is the curvilinear abscissa along the track length, the double dots identify a second-order derivative, m is mass, F_c is the force acting on the coupling systems, F_{tdb} is the force due to tractive/dynamic braking efforts, F_{air} is the contribution of air brake forces, F_{res} is the resistant force due to ordinary and curving resistances, calculated according to Equation (1) and finally F_g is the resistant force due to track slope. Please note that the traction/dynamic braking forces are non-zero on locomotives only, and that the air brake forces are neglected since the LTD benchmark input dataset did not consider air braking. The LTDPoliTo code calculates the in-train forces on the coupling elements from LUTs storing the force values as a function of deflection, with a smoothing transition function when the deflection speed is lower than a pre-defined threshold and a transition occurs between the loading and unloading curves, as suggested by Zhang et al.[29]

$$\begin{cases} F_c(\Delta x, \Delta v) = \begin{cases} F_L(\Delta x), & |\Delta v| \geq v_{ths} \wedge \Delta x \cdot \Delta v \geq 0 \\ F_U(\Delta x), & |\Delta v| \geq v_{ths} \wedge \Delta x \cdot \Delta v < 0 \\ F_M(\Delta x) + |F_A(\Delta x)| \dfrac{\Delta v}{v_{ths}}, & |\Delta v| < v_{ths} \end{cases} \\ F_M(\Delta x) = \dfrac{F_L(\Delta x) + F_U(\Delta x)}{2} \\ F_A(\Delta x) = \dfrac{|F_L(\Delta x) - F_U(\Delta x)|}{2} \end{cases} \tag{3}$$

where F_c is the force provided by the coupling system, Δx and Δv stand for deflection and relative speed, respectively, F_L and F_U are the LUTs storing the loading and unloading characteristics and finally v_{ths} is the threshold speed value, acting as defined above and set to 0.001 m/s in the simulations shown in the present paper. The LUTs defining the non-linear relationship between deflection and loading/unloading forces are defined according to data provided in the international benchmark [19] and are the same as those reported in references. [24,30–32]

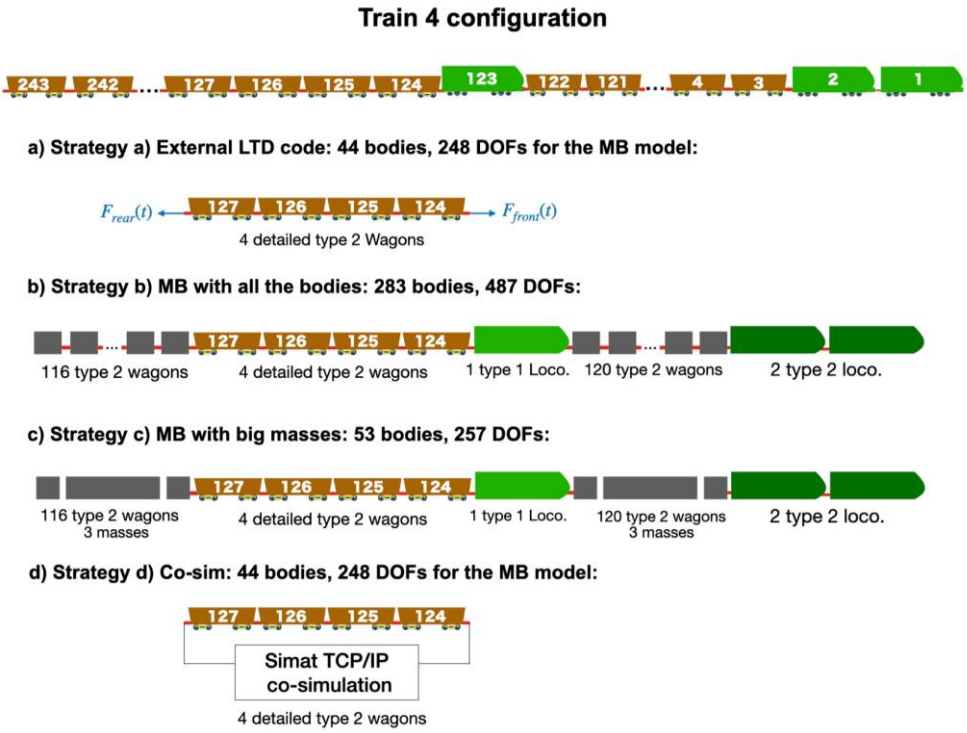

Figure 3 - Strategies for LTD simulation proposed by this work.

For every strategy proposed in this work, the four-car 3D MB model is positioned right behind the remote locomotive, where the largest in-train forces are produced.[20] Both MB and LTD models are solved through variable step-size predictor-corrector numerical integrators. Precisely, the MB model of the wagons is solved using the SODASRT2 solver [33], based on backwards differentiation formulas (BDFs) and suited for dynamic algebraic equation (DAE) systems, while the LTDPoliTo code relies on the ode15s solver available in MATLAB [34], which uses numerical differentiation formulas (NDFs), with preliminary specification of the Jacobian sparsity pattern. The use of variable step-size solvers is the key to adapt the step-size based on the conditions of the system under analysis and according to the estimation of the numerical error. The major parameters of the solvers, including the absolute and relative tolerances, were tuned and optimized in previous works for each base model.

Strategy a) is the easiest way to combine the effects of longitudinal and lateral dynamics in MB models because it imports the in-train forces from the outputs of an external LTD code, which in this paper is the LTDPoliTo code. The imported forces include the one acting between the remote locomotive and the first 3D wagon (F_{front}) and the force acting between the tail 3D wagon and the car behind (F_{rear}). As described before, this method fails to present the relationship between the MB forces and the LTD forces because the MB forces acting on the detailed cars do not affect the longitudinal forces generated previously.

Strategy b) allows to calculate all the in-train forces directly within the MB formalism, building in SIMPACK the entire pack of 243 cars included in train 4 configuration. Each car and locomotives are modelled as just one body each and are connected to the track using a follow track general rail joint with only the longitudinal (S) direction as a DOF. The four-3D car pack is then added to the train in positions 124 to 127. Just like the detailed wagons, each vehicle body in the model includes a dedicated force element to implement the expression in Equation (1) to account for the ordinary and curving resistances. For locomotives, the same approach is used to apply traction/dynamic braking, with the calculation of the force values based on the driving command and locomotive mechanical characteristics extracted from the international benchmark dataset. The connection between adjacent vehicles is modelled with SIMPACK default library elements for hysteresis behaviour ("Spr-Damp nonlin Hysts" SIMPACK force element), which implements a smoothing transition strategy similar to the one provided in Equation (2).

Strategy c) replaces each group of 1 DOF wagons with only 3 bodies with 1 DOF each. This approach simplifies calculations for estimating energy consumption or optimizing energy consumption and timetabling [35], but it cannot calculate in-train forces within the wagon pack. The wagon pack is split into three bodies: two 1 DOF cars ahead and behind the pack ("pivot" vehicles), and a central big mass. Clearly, this approach is not able to calculate the values of the in-train forces within the wagon pack, since the latter is modelled as a single point mass body. Nonetheless, when only focusing on the simulation of the detailed dynamics of a small group of well-defined wagons, this approach can easily account for the effect of the train composition at the cost of just adding a small number of bodies and DOFs. The connection between the big mass body and the pivot vehicles cannot be modelled with PtP hysteresis force elements, as during curve negotiation, the large overhang of the big mass body would produce numerical instabilities due to a huge length of the coupling element itself. Therefore, the connection between the central big mass and each pivot car is obtained with two pairs of additional forces, F_1 and F_2, that act as control forces to constrain the wagon pack to keep a constant length along the track curvilinear abscissa. In total, four additional force elements are defined, namely one force element on the pivot vehicle at the front, one force element on the rear pivot vehicle, and two force elements on the big mass body. The two forces acting on the big mass body have the same value in magnitude as the two forces on the pivot vehicles, but opposite direction to comply with the action-reaction principle, see forces F_1 and F_2 in Figure 4. For each pair of forces, one force element is defined between the pivot vehicle and the inertial reference system, while the other force, with the same value in magnitude, is applied between the big mass body and the inertial reference system. Precisely, the forces always act along the longitudinal direction, i.e., the direction that is tangent to the track centreline in each position. This is achieved by defining SIMPACK follow track connection/joint markers on the inertial reference system. These are special markers belonging to the reference system, that follow a body along the track curvilinear abscissa.

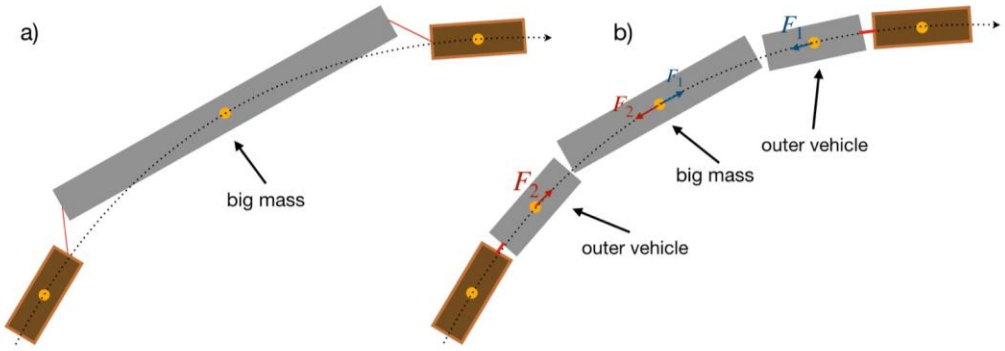

Figure 4 – Modelling of the big mass: a) overhang problem and b) addition of outer bodies and control force elements.

Each of the two pairs of forces F_1 and F_2 is calculated as:

$$F_i = K_p\left(S_{f,i} - S_{r,i} - S_{nom}\right) + K_c\left(\dot{S}_{f,i} - \dot{S}_{r,i}\right) \tag{4}$$

where subscript i can be either 1 or 2; S_f and S_r represent the position of the body in front and behind, respectively; the upper dot stands for derivative, S_{nom}, is the nominal distance between the bodies along the track curvilinear abscissa; and finally, K_p and K_c are control force element parameters. These parameters are tuned to obtain small errors in the wagon pack length during the simulation while, at the same time, not compromising the computational efficiency of the model. The values adopted in the simulations shown in this paper, which were identified through trial-end-error, are $K_p = 10^7$ N/m and $K_c = 5 \cdot 10^4$ Ns/m. For the pivot vehicles, the resistant forces are applied in the same way as for strategy b). For the central body, due to its large value of mass and length of the middle body, calculating the curving and slope resistant forces based on the position of its centre of gravity only would strongly modify the real train dynamics. Therefore, the curving and slope resistances for the central body are pre-calculated outside the MB environment considering the real mass distribution along the set, and they are indexed as a function of the position of the big mass centre of gravity in SIMPACK. Furthermore, an additional force must be applied to balance the longitudinal component of the middle body gravitational force when running on grades. This force is applied between the body reference frame marker and a follow track connection/joint marker on the inertial system along the longitudinal direction, and its value is calculated as:

$$F_{comp} = -g \cdot M_{big} \cdot Z'(S) \tag{5}$$

where g is gravity, M_{big} is the mass of the middle body and finally $Z'(S)$ is the slope along the track. The biggest benefit of this strategy is that it allows to consider the whole inertia of the train within the MB formalism with a small number of bodies and DOFs.

Strategy d) models the detailed pack of four-3D vehicles and obtains forces ahead and behind from a Simulink model with the LTDPoliTo code, using co-simulation. SIMPACK includes SIMAT, which enables co-simulation of the MB model with an external SIMULINK model via TCP/IP or S-functions. The main limitation is determining the sampling period, which is inversely proportional to the data exchange rate. A trade-off exists between accuracy and computational speed; larger sampling periods lead to accuracy loss. This paper investigates data transmission via the TCP/IP (Transmission Control Protocol/ Internet Protocol) protocol with communication rates of 0.1 ms and 0.01 ms. Please note that in the co-simulation architecture

selected in this work, the MB model still relies on the SODASRT2 solver, while the LTDPoliTo code implemented in SIMULINK is solved again with the ode15s solver. This means that each solver can independently adjust its own step-size during the simulation. However, data exchange is performed at discrete times depending on the communication period, which forces additional evaluations of the right-hand side terms and hinders from an increase of the step-size even when the errors are well below the tolerances.

The diagrams in Figure 5 illustrate communication and data exchange between LTD and MB codes for each strategy. For strategies b) and c), LTD is fully modelled within the MB framework, eliminating communication between LTDPoliTo and SIMPACK. For strategy a), LTDPoliTo runs a standalone simulation to obtain forces at the front and rear of detailed wagons, which are stored and inputted to SIMPACK. For strategy d), data exchange occurs at discrete time steps through TCP/IP, with LTDPoliTo feeding in-train forces and receiving wagon positions and velocities from SIMPACK.

For all strategies, the main simulation input is represented by the locomotive notch level, which is extracted from the international benchmark input dataset [19]. The notch level is provided as a function of the simulation time through indexing and interpolation of a dedicated LUT, which stores the time history of the driving command with a fixed step of 1 ms. Please note that the notch level characteristics is the only driving command input for the simulations shown in this paper, since the international benchmark only considers dynamic braking operations and does not include air brake applications. However, both the MB and LTD models could easily calculate air brake torques/forces by adding air brake modules implementing common literature approaches as reviewed in [36]. Other simulation inputs defined on all strategies are those related to the track layout, namely the track slope and curvature characteristics, which are given as a function of the position along the track curvilinear abscissa. During the simulation, curvature and slope are extracted by indexing specific LUTs storing data with a fixed track discretization step of 1 m. The discretization steps for both the notch level and track layout characteristics were optimized and tuned in previous activities dealing with the development and implementation of the LTDPoliTo code. [32]

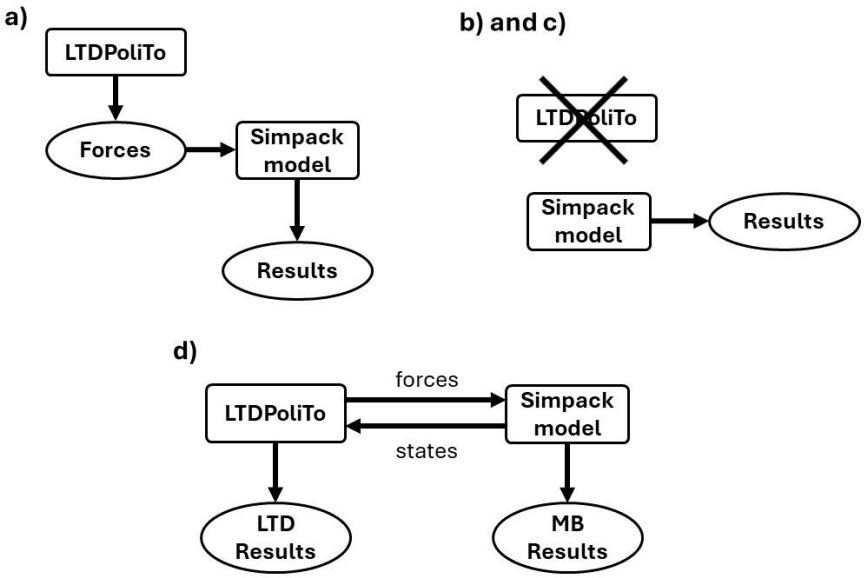

Figure 5 - Diagrams for each strategy's data exchange and results.

3. Results

All strategies shown in the section above are preliminary validated against the benchmark results [20] considering the speed profile, i.e., speed versus track location, for car 124, namely the car behind the remote locomotive, as shown in the train configuration sketched in Figure 3. This validation is essential to highlight any possible discrepancy among the strategies. Figure 6 shows the speed profile calculated with all four strategies, considering two sampling period values for strategy d) (co-simulation), i.e., 0.1 and 0.01 ms, corresponding to data exchange rates of 10 and 100 kHz, respectively. The benchmark results are presented in dashed black curve while the strategies are drawn in solid-coloured lines. For all strategies, the simulation time is set to the same value (3863 s), hence the final position along the track can differ due to discrepancies in the speed profile.

From Figure 6, all the strategies feature a good agreement in speed profile against the benchmark except strategy d), whose accuracy proves to be related to the sampling period between the Simulink and SIMPACK solvers. For the communication period of 0.1 ms, the speed profile starts to diverge around 4 km of simulation travel and the car tends to have a lower speed across the entire simulation. Around 27 km of simulation, the speed decreases by more than 10 km/h from the benchmark one, which causes the simulation to end before the end of the track since the simulation time was kept as the stop criteria. A smaller difference in speed is noticed in strategy d) when the communication period is reduced to 0.01 ms, thus confirming that small communication periods are needed to effectively capture the real train dynamics. On the other hand, strategies b) and c) are the most consistent with the benchmark, as they do not rely on data coming from other codes, and the MB models represent the inertia of the whole train. Finally, strategy a) shows a good level of consistency except for minor deviations seen around the 30 km mark and between 35 km and 40 km.

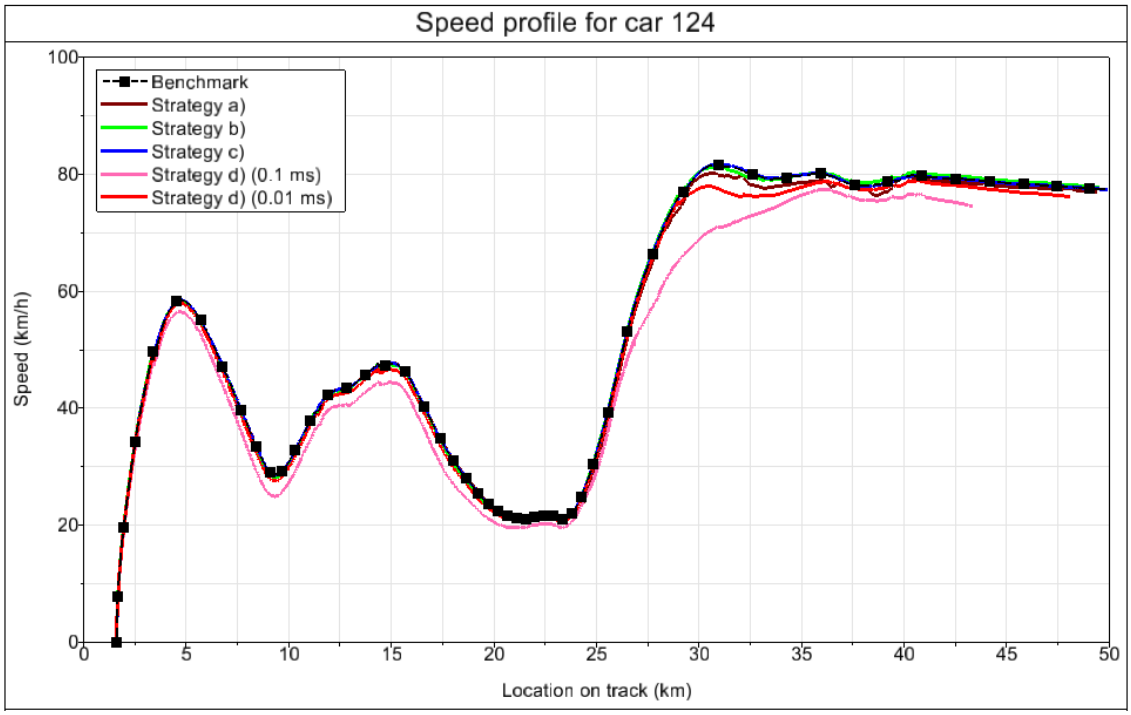

Figure 6 - Speed profile for car 124 along the track.

Similar considerations on the accuracy of the tested strategies can be made by observing the coupling forces generated between the wagons. Figure 7 shows the in-train forces on the coupling element connecting cars 123 and 124, found to be the highest coupling force generated in the entire composition, as described in [20]. The strategies align with the benchmark, except for the co-simulation strategy with a smaller communication rate (higher sampling period). Because of the delay observed in the position from Figure 6, the forces acting on the wagons deviate from the expected results, generating a higher level of buff forces around the 26 km mark and higher traction forces between the 30 km and 35 km marks. These higher forces explain the difference observed in the speed profile. Strategy d) with the communication rate of 0.01 ms also presents a smaller deviation from the other results between 30 km and 35 km marks but the model shortly regrouped with the benchmark. The reason for the discrepancies in the results calculated with co-simulation is mainly to be related to the driving command (locomotive notch) input, which is provided as a function of time according to the international benchmark of LTD simulators dataset. Consequently, small errors produced in the co-simulation due to bad convergence of the solvers lead to deviations in the speed profile, so that the driving command shifts in position with respect to the expected trend, thus further increasing the error, especially for large values of the sampling period.

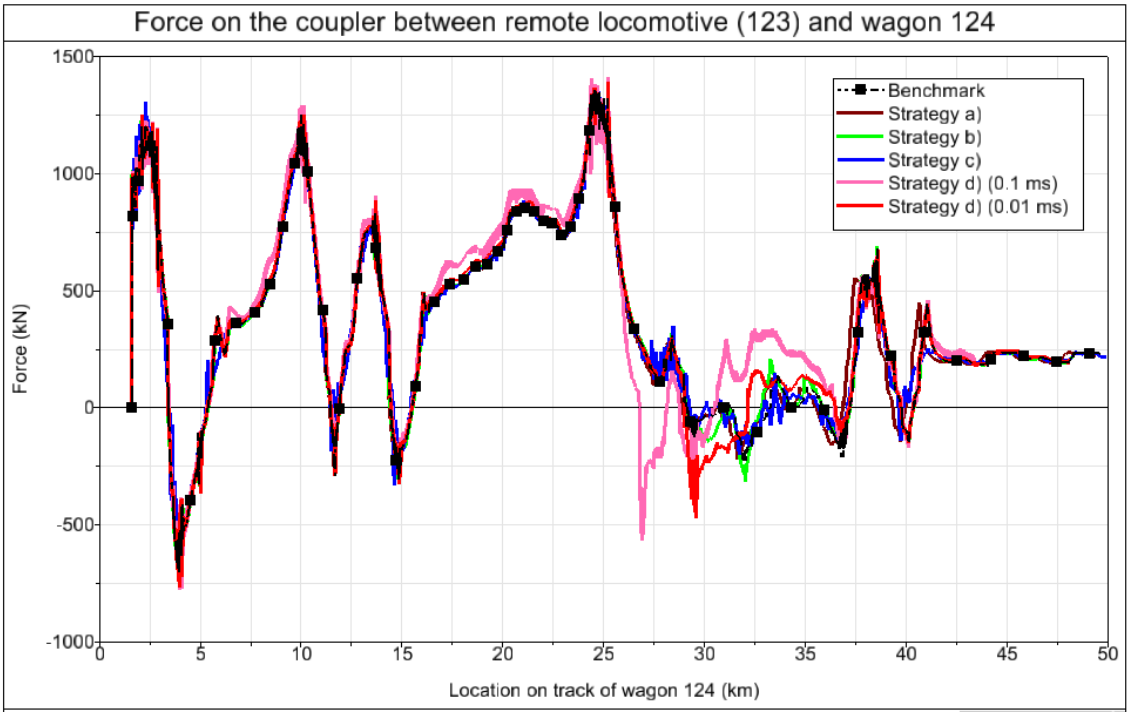

Figure 7 - Force acting on the coupler between cars 123 and 124 vs. the position of car 124.

The results shown above highlight the good agreement with the benchmark outputs for strategies, a), b), and c). The good accuracy of strategy c) proves the efficacy of the approach based on the application of the control force elements to keep a constant length of the wagon set, see Figure 4. For strategy d) (co-simulation), it is shown that a better agreement with all other strategies can be achieved if the sampling period is reduced from 0.1 ms to 0.01 ms, thus forcing additional data exchanges between the SIMULINK and SIMPACK environments. Residual discrepancies that appear around the 30 km mark can be related to the definition of the notch level as a function of time, so that possible deviations with respect to the theoretical speed profile generate additional cumulated errors. Unfortunately, a further refinement of the sampling period could not be tested due to the huge drop of computational times that this would cause.

As stated in the introduction, the major goal of this work is to investigate the effects of the tested strategies on the calculation of the running safety indexes. From each strategy, the Y/Q derailment coefficient is plotted for the two most critical curves, of 200 m of radius. Figure 8 shows the plot of the Y/Q parameter for the outer wheel on the leading wheelset of all 3D cars modelled, for strategies a), b) c) and d) only with 0.01 ms of communication rate, disregarding the results for the smaller communication rate, that proved to be unsatisfactory. For each strategy, the left part of the plot refers to the right-handed curve, while the right part of the plot refers to the left-handed curve. Strategies a) and d) have very similar results because the models are closer in their conceptions, having only the 4-car setup connected to an external code, with the forces acting ahead and behind coming from the LTD code and acting only on the running direction, thus not generating lateral components. On the other hand, for strategies b) and c), the forces acting on the head car, namely wagon 124, come from the connection to the locomotive. As the locomotive hangs more on the curve, this coupling element has a wider angle and generates a lateral component that affects the lateral forces on the wheel, creating the difference observed in both curves for the results of car 124. To get a further understanding of this effect, it would be necessary to develop a detailed model for the draft gear inside the MB model, severely increasing the model complexity. Other cars have very similar behaviours across all strategies.

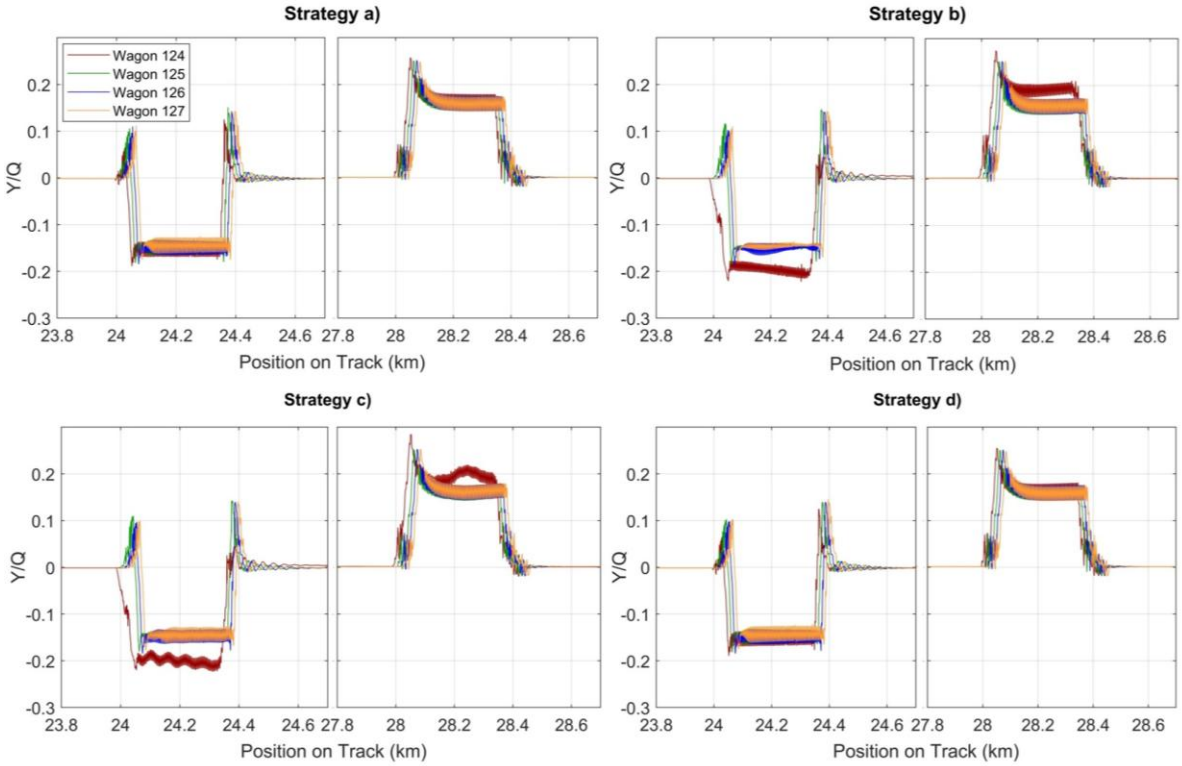

Figure 8 - Y/Q for outer wheels of leading wheelsets for each 3D wagon.

Car 124 also presents a dissimilar behaviour when comparing strategies b) and c). Strategy c) has a noisier characteristic with a vibration in the forces along the curves, which is caused by the control element used on the big masses representing the wagon block, not present in strategy b), which contains several bodies connected with multiple damping elements. The forces acting on car 127, the tail wagon of the group of detailed vehicles, are smaller. Hence, it is expected that less external effect is observed in this vehicle. Nonetheless, the results show that even for the most critical wagon (car 124), the derailment coefficient has limited variations when

changing the modelling strategies, thus confirming that all methods can be effectively adopted for a preliminary evaluation of the running safety indexes.

Finally, comparing the methods altogether, Table 2 presents the CPU time, wall clock time and real-time factor (RTF) recorded when launching the simulations with each strategy running on the same computer. The simulation computer features an AMD Ryzen 9 (7950x) processor with 16 cores and 32 GB of RAM. For each run, 6 physical threads are deployed while keeping the computer idle without other demanding tasks. The RTF presented in the table is the ratio between the wall clock time, i.e., the elapsed time since the beginning of the simulation, and the total simulation time, which is set to 3836 s for each strategy. RTF values below 1 mean the simulation runs faster than the real-time.

As shown in Table 2, strategy a) is the fastest, taking 639.79 seconds (10 minutes and 40 seconds) to execute, excluding measurements and previous LTD simulation time. Strategy b) doubles the number of DOFs and is about 7.4 times slower than a). Strategy c) is much faster than b) and only 14% slower than a) for the MB simulation. However, a) requires an additional computational time of 141 s, making c) even faster. Co-simulation strategies are slow due to communication between LTD and MB codes. With a 0.1 ms sampling period, it takes over a day (26 hours and 25 minutes), with an RTF of 24.632, much slower than real-time. However, a 0.1 ms sampling period leads to inconsistent results. Improving accuracy requires a 0.01 ms or lower sampling period, resulting in drastically slower performances (153 hours and 36 minutes, or 6 days!) and 143 times slower than real-time.

The slower computational speed of co-simulation (strategy d) is mainly due to the need for communication and data transfer between LTD and MB environments, which triggers different sources that contribute to the loss of computational performances. In fact, as the SIMAT block based on the TCP/IP protocol requires the definition of a fixed communication rate, the step-sizes selected by the ode15s solver for the LTD simulation and by the SODASRT2 solver for the MB model are always kept below the sampling period. This leads to extra evaluations of the right-hand side functions in both SIMULINK and SIMPACK environments. Furthermore, the SIMAT co-simulation requires the implementation of the LTDPoliTo code within SIMULINK, which does not enable a preliminary specification of the Jacobian sparsity pattern. This means that in failed steps, the solver calculates all elements in the LTD Jacobian matrix, with an additional increase of the computational times when compared to the standard implementation of LTDPoliTo in MATLAB. Finally, the communication itself between the SIMULINK and SIMPACK environments though the TCP/IP communication protocol contributes to an additional increase of the computational times. As the SIMAT block is a standard co-simulation interface between commercial software packages, it is not possible to obtain an estimate of the actual drop in computational performance given by each individual source, and only the overall increase of RTF is observed. Distributed computing could improve performance by running LTD and MB simulations on different computers, managing computational resources efficiently. However, this work compares simulations on the same computer for fairness. Higher efficiency could be achieved by developing customized co-simulation interfaces, as suggested by Spiryagin et al. [8], with the aim of reducing the simulation idle times and improving the convergence of the LTD and MB solvers.

Table 2 - CPU time, wall clock time and real-time factor for each strategy. The total simulated time is 3863 s and the times do not include measurements.

Strategy	CPU Time (s)	Wall clock time (s)	RTF real-time factor
Strategy a	3,678.531	639.790*	0.166
Strategy b	24,679.953	4,173.66	1.080
Strategy c	4,313.328	730.963	0.189
Strategy d *(0.1 ms)*	277,554.125	95,152.258	24.632
Strategy d (*0.01 ms*)	1,556,773.125	552,976.624	143.147

*Wall clock time does not include the time for LTD simulation with LTDPoliTo code, run previously

4. Conclusions

The simulations shown in this paper confirm that all tested literature strategies can lead to similar results and running safety indexes as calculated on the detailed wagons. Nonetheless, for co-simulation, accuracy proves to be strongly affected by the selected sampling period for data exchange between the LTD and MB code, thus generating a trade-off between accuracy and computational efficiency. The observed results have led to several conclusions, which are presented below in the form of a bullet list:

- Derailment coefficient varies minimally among strategies, with a minor influence from the methods used to apply in-train forces. For the selected simulation scenario, the derailment coefficient is well below the safety limits defined by the international standards. Future work should investigate detailed MB models of the coupling system.
- For the strategies that exchange data with LTD codes (strategies a) and d)), the forces in the longitudinal direction result in traction forces affecting speed profiles but omit lateral forces' impact than can be observed in strategies c) and d).
- Computational efficiency should guide strategy selection, as discrepancies in Real-Time Factor (RTF) arise among tested strategies.
- Strategy a) is the fastest, running six times faster than real-time (RTF = 0.166).
- Strategy b) uses detailed modelling but is slower than real-time (RTF = 1.08) due to its complexity.
- Strategy c) simplifies wagon packs as a much more efficient mass set, leading to just 14% slower performance than strategy a) but maintaining good efficiency (RTF = 0.189).
- Co-simulation is the slowest strategy, with accuracy strongly dependent on the data exchange rate between environments. The co-simulation architecture investigated in the present paper is the SIMAT block, relying on TCP/IP connection. Future upgrades of the activity should assess the influence of different communication protocols and architecture, which could improve the co-simulation performances.

It should be noted that certain aspects of railway simulation, including worn wheel and rail profiles, wheel-rail friction variation, track irregularities and defects, traction and braking forces, are beyond the scope of this work, as forementioned, and therefore not addressed in the conclusions.

Acknowledgement

The authors wish to express their acknowledgement to Vale S.A. for partially funding this study and for technical support. Also, to CNPq (grant number 303582/2023-5), which funded A. A. Santos and CAPES (grant number 88887.892546/2023-00) which funded P. H. A. Correa.

Statements and declarations

The authors declared no potential conflicts of interest with respect to the research, authorship, and/or publication of this article. This article does not contain any studies with human or animal participants.

Data Availability

The data obtained in this study isn't publicly shared. The data used as inputs are present on different other works cited along the work. The generated results are available only to the authors and collaborators. Requests for access can be considered individually with proper reasoning and approval.

Credit Statement

M. Magelli: conceptualization, methodology, modeling, software, writing (original draft and revised version), data investigation; **P. H. A. Correa:** conceptualization, methodology, modeling, writing (original draft), proofreading (original draft and revised version), data investigation, image generation; **A.A. Santos**: conceptualization, writing - review & editing, supervision.

References

1. Shabana AA. *Dynamics of Multibody Systems*. Cambridge University Press, 2005. Epub ahead of print 2 May 2005. DOI: 10.1017/CBO9780511610523.

2. Wu Q, Spiryagin M, Cole C. Longitudinal train dynamics: an overview. *Vehicle System Dynamics* 2016; 54: 1688–1714.

3. Spiryagin M, Cole C, Sun YQ, et al. *Design and Simulation of Rail Vehicles*. CRC Press. Epub ahead of print 13 May 2014. DOI: 10.1201/b17029.

4. Bosso N, Gugliotta A, Zampieri N. A Mixed Numerical Approach to Evaluate the Dynamic Behavior of Long Trains. *Procedia Structural Integrity* 2018; 12: 330–343.

5. Corrêa PHA, Ramos PG, Teixeira LHS, et al. Dynamic simulation of a heavy-haul freight car under abnormal braking application on tangent and curve. *Vehicle System Dynamics*. Epub ahead of print 2022. DOI: 10.1080/00423114.2022.2113807.

6. Bracciali A, Megna G. Track friendliness of an innovative freight bogie. In: Li Z, Nunez A (eds). Delft, The Netherlands: TUDelft, 2018.

7. Belforte P, Cheli F, Diana G, et al. Numerical and experimental approach for the evaluation of severe longitudinal dynamics of heavy freight trains. In: *Vehicle System Dynamics*. 2008, pp. 937–955.

8. Spiryagin M, Simson S, Cole C, et al. Co-simulation of a mechatronic system using Gensys and Simulink. *Vehicle System Dynamics* 2012; 50: 495–507.

9. Wu Q, Spiryagin M, Cole C, et al. Parallel computing in railway research. *International Journal of Rail Transportation* 2020; 8: 111–134.

10. Bosso N, Zampieri N. Numerical stability of co-simulation approaches to evaluate wheel profile evolution due to wear. *International Journal of Rail Transportation* 2020; 8: 159–179.

11. Wu Q, Spiryagin M, Liu P, et al. Co-simulation methods for train braking dynamics. *Proc Inst Mech Eng F J Rail Rapid Transit* 2023; 237: 1072–1081.

12. Spiryagin M, Wu Q, Cole C, et al. Advanced studies on locomotive dynamics behaviour utilising co-simulation between multibody and train dynamics packages. *Conference on Railway Excellence (CORE2016)*, https://acquire.cqu.edu.au/articles/conference_contribution/Advanced_studies_on_locomotive_dynamics_behaviour_utilising_co-simulation_between_multibody_and_train_dynamics_packages/13434761 (2017).

13. Pogorelov D, Yazykov V, Lysikov N, et al. Train 3D: the technique for inclusion of three-dimensional models in longitudinal train dynamics and its application in derailment studies and train simulators. *Vehicle System Dynamics* 2017; 55: 583–600.

14. Cantone L, Negretti D, Vullo V. Evaluation of the Admissible Longitudinal Compressive Forces by Means of Multibody Train Simulations. In: Pombo J (ed). Civil-Comp Press, 2012. Epub ahead of print 2012. DOI: 10.4203/ccp.98.26.

15. Bosso N, Zampieri N. Long train simulation using a multibody code. *Vehicle System Dynamics* 2017; 55: 552–570.

16. Magelli M, Zampieri N. A novel approach for longitudinal train dynamics simulations with multibody codes. *Vehicle System Dynamics*. Epub ahead of print 2024. DOI: 10.1080/00423114.2024.2362949.

17. Bernal E, Wu Q, Spiryagin M, et al. Augmented digital twin for railway systems. *Vehicle System Dynamics* 2024; 62: 67–83.

18. Bosso N, Magelli M, Zampieri N. Application of machine learning techniques to build digital twins for long train dynamics simulations. *Vehicle System Dynamics* 2023; 62: 21–40.

19. Spiryagin M, Wu Q, Cole C. International benchmarking of longitudinal train dynamics simulators: benchmarking questions. *Vehicle System Dynamics* 2017; 55: 450–463.

20. Wu Q, Spiryagin M, Cole C, et al. International benchmarking of longitudinal train dynamics simulators: results. *Vehicle System Dynamics* 2018; 56: 343–365.

21. Pacheco P, Lopes MV, Correa PHA, et al. Influence of Primary Suspension Parameters on the Wear Behaviour of Heavy-Haul Railway Wheels Using Multibody Simulation. In: *International Conference on Electrical, Computer, Communications and Mechatronics Engineering, ICECCME 2023*. Institute of Electrical and Electronics Engineers Inc., 2023. Epub ahead of print 2023. DOI: 10.1109/ICECCME57830.2023.10252905.

22. Corrêa PHA, Ramos PG, Fernandes R, et al. Effect of primary suspension and friction wedge maintenance parameters on safety and wear of heavy-haul rail vehicles. *Wear*; 524–525. Epub ahead of print 15 July 2023. DOI: 10.1016/j.wear.2023.204748.

23. de Paula Pacheco PA, Magelli M, Lopes MV, et al. The effectiveness of different wear indicators in quantifying wear on railway wheels of freight wagons. *Railway Engineering Science*. Epub ahead of print 2024. DOI: 10.1007/s40534-024-00334-8.

24. Bosso N, Magelli M, Rossi Bartoli L, et al. The influence of resistant force equations and coupling system on long train dynamics simulations. *Proc Inst Mech Eng F J Rail Rapid Transit* 2022; 236: 35–47.

25. Wu Q, Wang B, Spiryagin M, et al. Curving resistance from wheel-rail interface. *Vehicle System Dynamics* 2022; 60: 1018–1036.

26. Ayasse JB, Chollet H. Determination of the wheel rail contact patch in semi-Hertzian conditions. *Vehicle System Dynamics* 2005; 43: 161–172.

27. Quost X, Sebes M, Eddhahak A, et al. Assessment of a semi-Hertzian method for determination of wheel-rail contact patch. *Vehicle System Dynamics* 2006; 44: 789–814.

28. ABNT. *NBR 16810: Via férrea - Superelevação em curvas.," Associação brasileira de normas técnicas*. Rio de Janeiro, 2019.

29. Zhang Z, Li G, Chu G, et al. Compressed stability analysis of the coupler and buffer system of heavy-haul locomotives. *Vehicle System Dynamics* 2015; 53: 833–855.

30. Bosso N, Magelli M, Zampieri N. Development and validation of a new code for longitudinal train dynamics simulation. *Proc Inst Mech Eng F J Rail Rapid Transit* 2021; 235: 286–299.

31. Bosso N, Magelli M, Zampieri N. Validation of a new longitudinal train dynamics code for time domain simulations and modal analyses. *International Journal of Transport Development and Integration* 2021; 5: 41–56.

32. Bosso N, Magelli M, Zampieri N. Long train dynamic simulation by means of a new in-house code. *WIT Transactions on the Built Environment* 2020; 199: 249–259.

33. Brenan KE, Campbell SL, Petzold LR. *Numerical solution of initial-value problems in differential-algebraic equations*. Society for Industrial and Applied Mathematics, 1987.

34. Shampine LF, Reichelt MW, Sci Comput SJ. *THE MATLAB ODE SUITE* *, http://www.siam.org/journals/ojsa.php (1997).

35. Scheepmaker GM, Goverde RMP, Kroon LG. Review of energy-efficient train control and timetabling. *European Journal of Operational Research* 2017; 257: 355–376.

36. Wu Q, Cole C, Spiryagin M, et al. Freight train air brake models. *International Journal of Rail Transportation* 2023; 11: 1–49.